JAEA-Review

**In-Core Integrity of the 4.8gU/cc Silicide Fuels
Fabricated by B&W and CERCA**

Kazuaki YANAGISAWA

Policy Planning and Administration Department

# In-Core Integrity of the 4.8gU/cc Silicide Fuels
# Fabricated by B&W and CERCA

Kazuaki YANAGISAWA

Policy Planning and Administration Department, Japan Atomic Energy Agency,
Watanuki-machi, Takasaki-shi, Gunma-ken

The silicide fuel fabricated by B&W (one T/C) and that fabricated by CERCA (no T/C) was pulsed with the reactivity of 1.43 dollar ($). The energy deposition was 115 cal/g・fuel plate for the former and 98 cal/g・fuel plate for the latter. In-core transient fuel performance of the two was directly compared, using the data obtained from 4.8g/cc silicide fuels as the references. (1)The onset of DNB temperature for the B&W fuel was 154 deg. C, which was the lowest among the references having DNB of 182±18 deg. C. (2) During the quenching, the B&W fuel had 269 deg. C for the temperature difference $\Delta T$ (>94 deg. C for failure) and 0.079s for the time to quench tq (<0.13s for failure). This situation brought the quench failure to the fuel. The failure mode was the through-plate cracking occurred near the T/C#1 and the incipient cracking occurred near the fuel top region. The CERCA fuel did not fail not telling the details due to the no in-core instrument (3) The B&W fuel bowed to the magnitude of 34%, enhanced by the high PSCT by 391 deg. C. The CERCA fuel bowed to the magnitude of only 6%, perhaps associated with the comparative low PCST. (4) The residual strain for the both cases was in the range of ±5%, showing the similarity to that of the references. (5) As the typical abnormality, the B&W fuel caused the local hot spot and the pitting in the Al-3wt% Mg cladding.

Keywords: Silicide Fuel, Failure Threshold, Failure Mechanism, Departure from the Nucleate Boiling (DNB), Time to Quench, Temperature Difference, Through-plate Cracking, Bow, Residual Strain

# B&W および CERCA 社で作製された 4.8gU/cc シリサイド燃料の炉内健全性

日本原子力研究開発機構経営企画部

栁澤　和章

B&W 社で作製したシリサイド燃料（熱電対 1 本付き）及びセルカ社で作製したシリサイド燃料(熱電対無)を、ともに投入反応度 1.43 ドル($)でパルス照射した。得られた発熱量は前者が 115 cal/g・fuel plate で、後者が 98 cal/g・fuel plate であった。両者に関する炉内燃料過渡性能を直接比較するとともに、実施済みの 4.8g/cc シリサイド燃料の過渡性能を比較用レファレンスとして使用した。(1)B&W 社製の燃料に関する核沸騰離脱温度（DNB）は 154℃であり、レファレンスが有する DNB 温度の 182±18 ℃と比較して低かった。(2)クエンチ時、 B&W 燃料はクエンチ温度差 ΔT として 269℃(>94℃、破損しきい値)を示し、クエンチ時間 tq として 0.079 秒(<0.13 秒、破損しきい値)を示した。このような状況で燃料は破損に至った。破損様式は燃料板貫通割れで溶接熱電対#1 の近傍で発生していた。また、未貫通割れが燃料板上部近傍で発生した。CERCA 社製燃料板は破損しなかったが、炉内計装が何も無かったため破損メカニズムに関する議論が出来ない。(3) B&W 社製の燃料板には 34%の曲がりが発生したが、これは燃料被覆表面最高温度（PCST）が 391℃と高かったためである。CERCA 社製の燃料板は僅か 6%の曲がりであった。曲がりと PSCT は比例するので、CERCA 社製の燃料板の PCST は相対的に低かったと推察する。(4) 両者の燃料板残留歪は±5%の範囲内にあり、レファレンスと同等レベルだった。(5)典型的な形態異常として、B&W 燃料の Al-3wt% Mg 被覆材に、局所的なホットスポットとピッティングが見られた。

高崎量子応用研究所（駐在）：〒370-1292　群馬県高崎市綿貫町 1233

Contents

目次

# 1 Introduction

In the author's previous studies [1-11], the failure threshold of the un-irradiated silicide mini-plate fuel (4.8g/cc) was discussed and decided experimentally. The failure would occur, when the fuel had the low time to quench (<0.13s) and the high temperature drop (>94 deg. C). The thermal stress was the principal mechanism led by the uneven temperature profiles across the fuel plate. In the present study, the 12907030 specimen fabricated by the B&W and the CS514836 specimen fabricated by the CERCA were prepared for the pulsed irradiation of Ex.508-13 and that of Ex. 508-11. In order to make a direct comparison between the two, the same reactivity of 1.43 dollar was designed to give to each, the reactivity was corresponded to the energy deposition of 94 cal/g・fuel plate where the quench failure occurred usually . One of the unique features used in the study was the number of T/C, hence, the B&W fuel had only one T/C spot welded to the Al-cladding and the CERCA fuel had no T/C. The data points of the 4.8g/cc silicide fuels obtained from the previous studies [1-11] were used as the references since they had six to nine T/C's.

# 2 Experiment

## 2.1 Characteristics of the test specimen
(1) Dimension
The test mini-plate fuels or the test specimens used in the present study were designed by the Japan Atomic Energy Research Institute (JAERI). A schematic of the 12907030 specimen with one T/C is shown in **Fig. 1.** It was fabricated by the B&W in Virginia, the U.S. Another CS514836 specimen with no T/C was fabricated by the CERCA in Romans, France. They consisted of the fuel core (25mm width×70mm length×0.51mm thickness) sandwiched by the Al-3wt%Mg alloy based cladding (35mm width×135mm length×1.27mm thickness, hereinafter abbreviated Al-cladding). A dimensional comparison of the test specimen with the Japan Materials Testing Reactor (JMTR) full-scale plate fuel showed that the core and the plate sizes of the former are 1/5-1/2 of the latter except for the thickness. The situation is almost the same as those of the JRR-3 full-scale plate fuels.
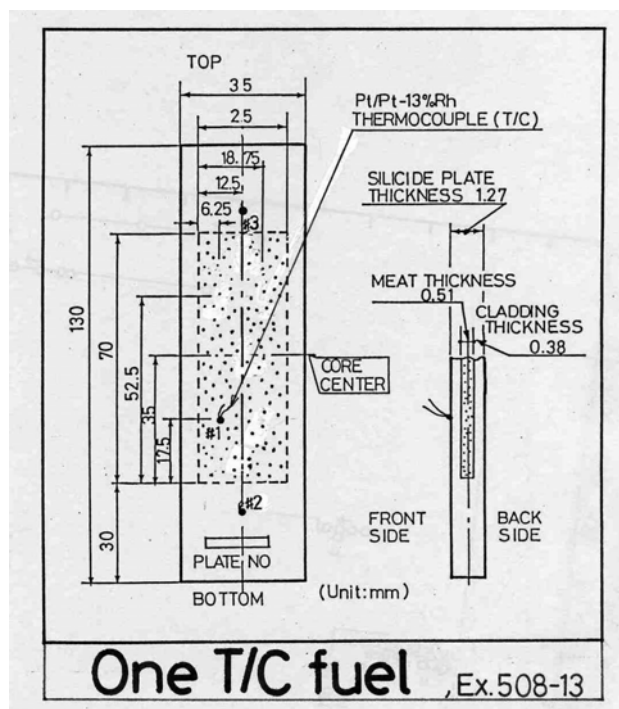
Figure 1: The schematic presentation of the 4.8g/cc silicide mini-plate fuel, having one T/C at the #1 location. The 12907030 specimen having the enrichment by 19.76 wt% [235]U was fabricated by the B&W and used in the experiment 508-13

(2) Fuel characteristics

The major characteristics of the test specimen are summarized in **Table 1.** The test specimens had uranium (U) density by 4.8g/cc, the same as those of the references. In the study, the total of 12 references was prepared. Details of the references were described elsewhere [4]. Additionally, the experimental number and the deposited energy of the references were described in the Table 2 shown in the later on.

Table 1 Characteristics of the test specimen used in the present study

| 1. Silicide core　（U-21wt%Al-7.5wt%Si） | | |
|---|---|---|
| Test specimen | CS514836 | 12907030 |
| Experiment | 508-11 | 508-13 |
| Thermocouple （T/C） | No | One |
| （1）Dimension　（mm） | 70　（length）　x 25　（width）　x 0.51　（thickness） | |
| （2）Enrichment　（wt%） | 19.95 | 19.76 |
| （4）U density (g/cc) | 4.8 | |
| （3）Si（wt%） | 7.5 | 7.7 |
| （5）Void fraction　（%） | 5 | 6.3 |
| （6）Fuel composition | U3Si2+USi, U3Si2 density :12g / c.c., U3Si2 > 97wt% | |
| （7）Matrix | A5NE　（Al-0.3wt%Fe） | A6061-0 |
| 2. Aluminum alloy cladding | | |
| （1）Dimension　（mm） | 130　（length）　x 35　（width）　x 1.27　（thickness） | |
| （2）Composition | Al-2.8wt%Mg　（AG3NE） | Al-1.0wt%Mg　（A6061-0） |
| （3）Density　（g/c.c.） | 2.67 | |
| （4）Tensile strength　（MPa） | 240 | 114 |
| （5）0.2% proof strength（MPa） | 130 | 62 |
| （6）Elongation　（%） | 25 | 29 |
| （7）Blister test | No blister at annealing temperature of 475℃, >1h | |

2.2　　Instrumentation and irradiation capsule

The in-core instrumentation was Pt/Pt-13%Rh bare wire thermocouples　（0.2mm outer diameter）, hereinafter abbreviated as "T/C's" with a melting point of 1,780 deg. C. As shown in **Fig. 1**, it was directly spot welded to the external surface of the Al-3wt%Mg cladding at the T/C#1 location in the experiment 508-13 (B&W fuel). However, no T/C was welded in the experiment 508-11(CERCA fuel). The references had the T/C's up to 9, in which T/C#8 was welded in a no-fuel region. At the assembling stage, the test specimen was attached to the supporting jig with electric cables and was loaded into an irradiation capsules as shown schematically in **Fig. 2**. The irradiation test with this instrumentation was conducted in the stagnant water at room temperature of about 20 deg. C and one atmospheric pressure inside the sealed irradiation capsule.
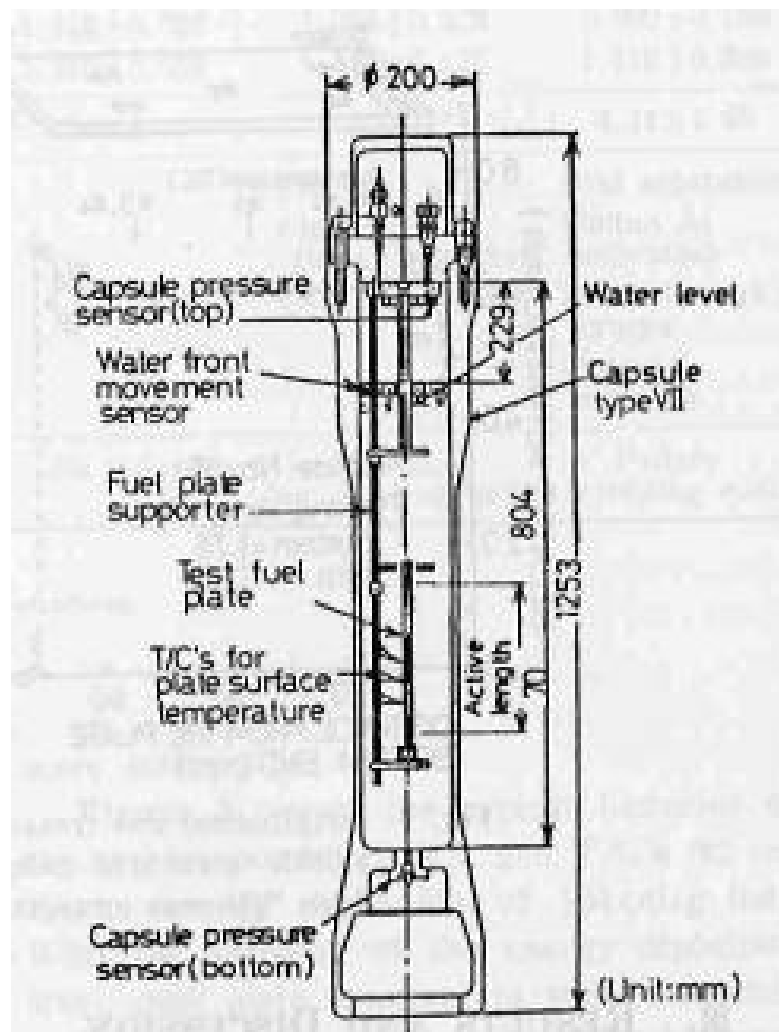
Figure 2: A schematic drawing of the NSRR irradiation capsule designed for the in-core power transient test

## 2.3　Pulse history

(1) Pulse history

All tests including the test specimens were conducted with a single plate configuration. Generally, the half-width power of the Nuclear Safety Research Reactor (NSRR) pulse irradiation is a minimum of about 4.4ms at a maximum integral power of 110MW・s. The value of this width varies from 4.4 to 20ms depending on the magnitude of the inserted reactivity.

(2) Power skew

The power profile of the test specimen was almost flat in the two directions except at the end, where the power was about 8% higher than average. The power profile at each

T/C in the test specimen was uniform at the post-irradiation examination (PIE), but might be not during irradiation. As will be mentioned below, the temperature distribution across the fuel plate should be uneven. This will accompany the irregular shape of the quench front during the course of temperature quenching. The local sharp peaks at the end of the fuel core were principally due to the boundary existing between the enriched and non-enriched fuel core regions and occasionally due to the uneven shape of the core tail, which occurred during the rolling process when the fuel plate was fabricated.

(3) Transient temperature

The transient temperature is the common to all test specimens and the references. In **Fig. 3**, as an example, a typical transient temperature obtained from one of the references (T/C #4, experiment 508-8) that received an energy deposition of 97 cal/g・fuel plates is shown with the pulse power as indicated by the dotted line. The fuel temperature behaved as follows. The cladding surface temperature (CST) exceeded the boiling temperature, $T_i$ （154 deg. C）, beyond the saturation temperature, $T_{sat}$ （100 deg. C）, due to the pulse irradiation. The commencement of the coolant boiling at the temperature $T_i$ was determined by the data obtained from a capsule water level sensor. Namely, the timing of the coolant boiling was detected by the movement of water free surface, and the timing of water free surface movement was detected by the floating buoy having a magnetic sensor inside. The CST continued to increase to an overshoot temperature, $T_{ov}$ （203 deg. C）. It then decreased to 194 deg. C and remained <10ms.
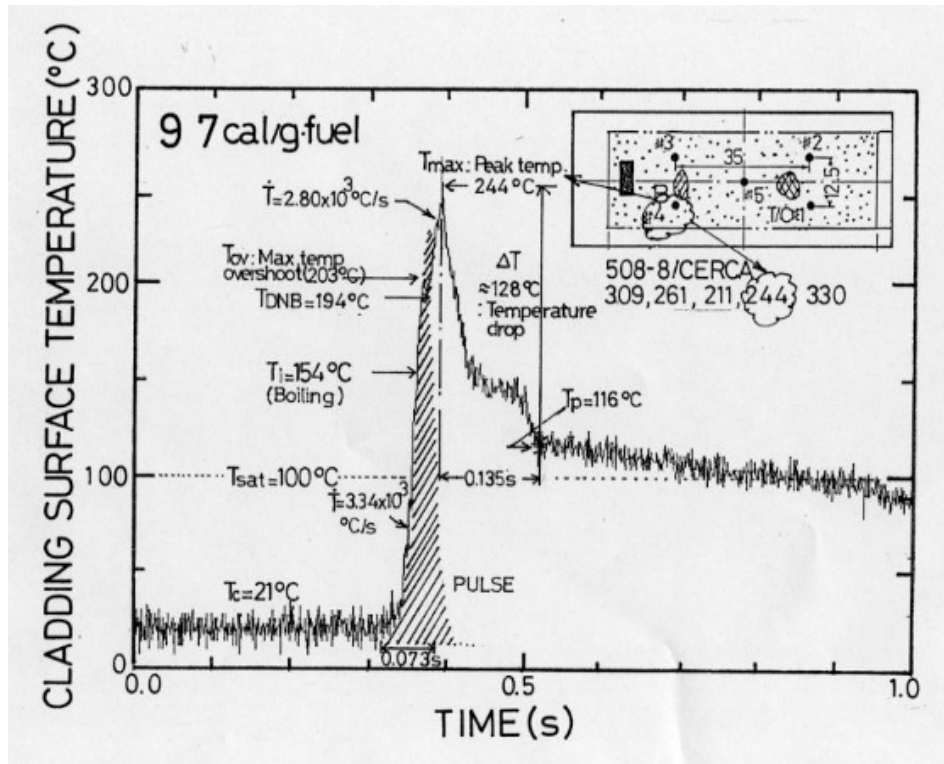
Figure 3: Typical example of cladding surface temperature （solid line ）and reactor power（dotted line）, showing boiling temperature （$T_i$）, DNB temperature （$T_{DNB}$）, maximum overshoot temperature （$T_{ov}$）, peak cladding surface temperature （$T_{max}$）, quench temperature （$T_p$）, temperature drop（$\Delta T$）, and time to quench （$t_q$）. These are from T/C #4 of the mini-plate fuel used in experiment 508-8 （97 cal/g・fuel plate, failure）.The location of the TC is schematically shown in the top right.

This CST was thought to be the commencement of the film boiling. The author denoted it as $T_{DNB}$ and denoted here as the (onset of) DNB temperature. A signal of the DNB temperature can be detected from a temperature plateau that should appear after $T_{ov}$. The value of the onset of the DNB obtained from the test specimen was 182±15 deg. C from the average of 53 data points. Above the $T_{DNB}$, the increase in the CST terminated at the $T_{max}$ （244 deg. C） or the peak cladding surface temperature (PCST). The CST was then quenched to temperature $T_p$ （116 deg. C） during the interval of $t_q$ （0.135s）. The magnitude of the temperature difference given by $\Delta T = T_{max} - T_p$ is denoted here as the "temperature drop $\Delta T$（128 deg. C for this case）". Note that PCST measured during the course of the experiments is almost above $T_{DNB}$.

(4) Fin effect of T/C

In two experiments (Ex.508-4 and Ex.508-5) done by the references, all the PCSTs further exceeded the melting point of the Al cladding. **Figure 4** shows the typical

transient temperature around the melting point observed in the Ex.508-4. The measured melting point of the Al cladding was found to be 579±36 deg. C, an average from 10 T/C's. It was lower than that（573～640 deg. C）given by the binary phase diagram, due to the fin effect of the T/C's. As can be seen here, the magnitude of the fin effect was about 61±36deg C. It is important for the quench failure mechanism whether or not the fin effect could be assisted a formation of the uneven temperature profiles across the test fuel plate. The principal aim of the B&W fuel (one T/C) and CERCA fuel (no T/C) was addressed to this matter. Then, the author put the same reactivity of 1.4$ to them, however, this intention was in failure because the resultant energy deposition was 115 cal/g・fuel plate for the former and 98 cal/g・fuel plate for the latter.
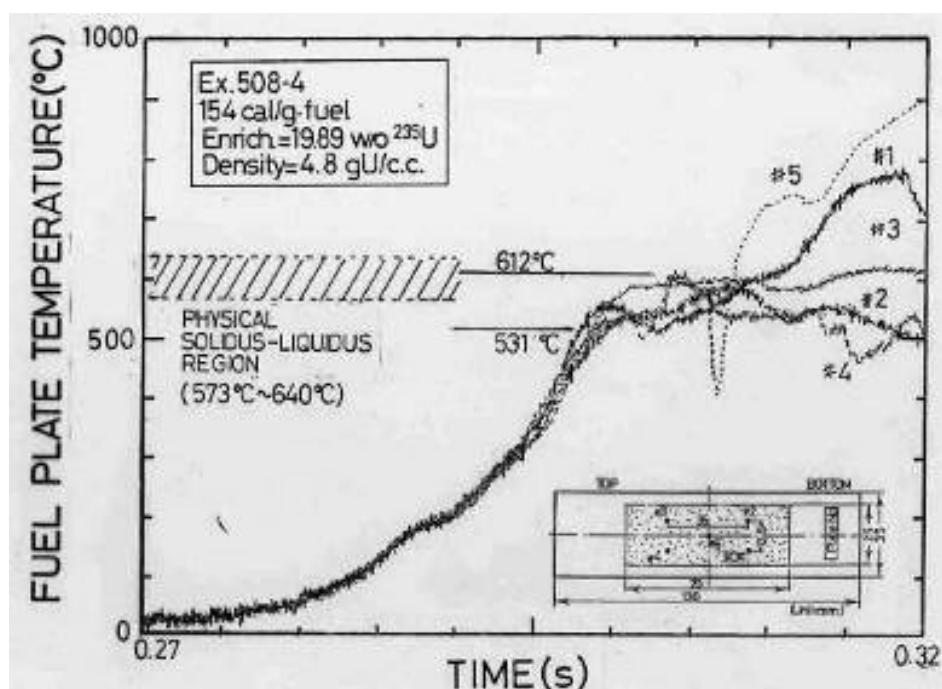


Figure 4 The solidus-liquidus transformation temperatures of the Al-3wt%Mg alloy （AG3NE）observed in the experiment 508-4. The measurement was carried out by the T/C's welded directly to the Al cladding surface. The physical solidus-liquidus transformation temperatures cited from a binary phase diagram of the Al-3wt%Mg alloy are shown by the hatched area.

## 3        Results and Discussion

In **Table 2**, for the reader's convenience all data obtained from the in-core measurements and the PIE is summarized. In addition to the experiments (Ex.) 508-13 and 508-11, a total of 11 experiments obtained from the references were included. In the subsequent sections, the discussion will be made according to numerals taken from this table.

### 3.1 The deposited energy

As seen in the **Table2**, the four reference fuels, that is, CS514831 (Ex.508-6), 12907010 (Ex.508-7), CS514832 (Ex.508-8) and CS514834 (Ex.508-9) were pulsed with the reactivity of 1.43, 1.43, 1.43 and 1.49 dollar ($) in order to study the failure threshold and the failure mechanism. The deposited energy of those was respectively 96, 94, 97 and 95 cal/g・fuel plate, where all the fuels failed. Taking this fact into consideration, the author prepared the CS514836 (Ex.508-11, CERCA, no T/C) and 12907030 (Ex.508-13, B&W, one T/C) to give the same reactivity by 1.43$. The deposited energy after burn-up analysis, however, was 98 cal/g・fuel plate for the former and 115 cal/g・fuel plate for the latter. Despite the same reactivity insertion, the resultant energy deposited to the test specimen was different. However, this confliction was not the first case. In the aforementioned test done by CS514834 (Ex.508-9), the energy deposition of the 95 cal/g・fuel plate was produced by the reactivity of 1.49$. The author did not understand whether or not the use of the silicide fuel from the different vendors was the main cause of this confliction. Another surprise was that the CS514836 (no T/C) at 98 cal/g・fuel plate did not fail, though the value was higher than that of the failure threshold of 94 cal/g・fuel plate, though it was also not the first case. Not described detail in this paper, CS514009 silicide specimen having 4.0g/cc was pulsed with 106 cal/g・fuel plate but did not fail. At that case the specimen had 9 T/C's. It should be said that the energy deposition is not the deterministic factor for the quench failure. Due to the reason, the author would prefer to use the temperature difference ΔT and the time to quench tq as the important parameters for the quench failure mechanism, as described in the subsequent sections.

### 3.2 The visual inspection of the test specimen

After dismantling the test specimens from the irradiation capsule and jig, the author made the visual inspections to confirm the integrity of the test specimens. In **Photo.1**,

an overview of the test specimen used for Ex.508-11 (no T/C) and that used for Ex.508-13 (one T/C) are shown. For the former, there existed no abnormalities except for the water crud, deposited when the test specimen was cooled in the fuel pit for one month. For the latter, the author observed two abnormalities, one was the though-plate cracking located near the T/C#1 and the other was the incipient cracking located at the fuel top region. Hence, the test specimen without T/C did not fail but the test specimen with one T/C failed.
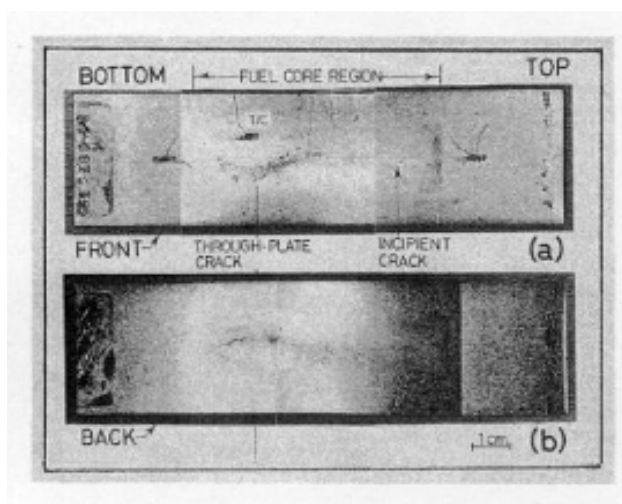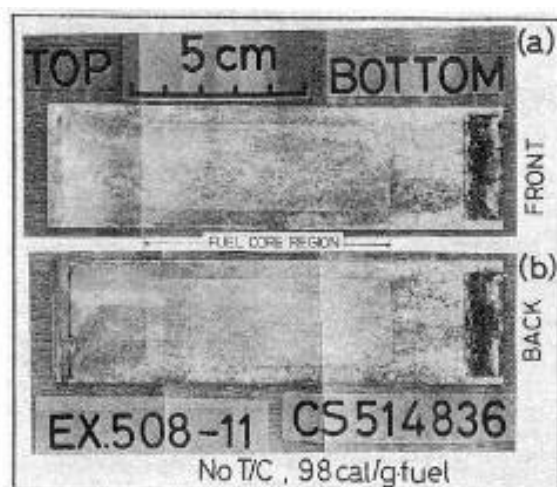


Photo.1 An overview of the test specimen; (top) no T/C fuel plate used in Ex.508-11 and (bottom) one T/C fuel plate used in Ex.508-13, where the T/C#1 was spot welded to the fuel active (enriched) core region in the Al-3wt%Mg cladding and two T/C's were spot welded in the non-fuel (cold) region to have a referential data.

Table 2 Summary of in-core measurements and data obtained from PIE; Ex.508-11(CERCA, no T/C), 508-13(B&W, one T/C) and 11 references

| Table 2 Experiment | Test specimens | | Reference fuels | | | | | | | | | | |
|---|---|---|---|---|---|---|---|---|---|---|---|---|---|
| | 508-11 | 508-13 | 508-1 | 508-2 | 508-3 | 508-4 | 508-5 | 508-6 | 508-7 | 508-8 | 508-9 | 508-10 | 508-12 |
| Miniplate fuel number | CS514836 | 12907030 | CS514815 | CS514816 | CS514819 | CS514829 | CS514830 | CS514831 | 12907010 | CS514832 | CS514834 | 12907020 | CS514837 |
| Fuel type | | | | | | | Silicide | | | | | | |
| Deposited energy (cal/g·fuel plate) | 98 | 115 | 62 | 77 | 116 | 154 | 164 | 96 | 94 | 97 | 95 | 82 | 32 |
| Fuel density (g/cc) | | | | | | | 4.8 | | | | | | |
| Fuel enrichment (wt %) | 19.95 | 19.76 | 19.86 | 19.86 | 19.91 | 19.86 | 19.81 | 19.86 | 19.76 | 19.86 | 19.99 | 19.76 | 19.86 |
| Number of thermocouples at enriched plate | 0 | 1 | 6 | 5 | 5 | 5 | 5 | 5 | 5 | 5 | 7 | 7 | 9 |
| Peak cladding surface temperature (°C) #1 | NoT/C | 391 | x{a} | 200 | 350 | 971 | 779 | 270 | 198 | 309 | 279 | 216 | 133 |
| #2 | - | - | 177 | 179 | 372→387 | 893 | 689 | 229 | 210 | 261 | 315 | 180 | 136 |
| #3 | - | - | 216 | 183 | 414 | 652 | x | 202 | 199 | 211 | 284 | 227 | 136 |
| #4 | - | - | 234 | 178 | 393 | 881 | 918 | x | 237 | 244 | 285 | 173 | 134 |
| #5 | - | - | 178 | 195 | 424→544 | 930→957 | 578→656 | 205 | 191 | 330 | 305→261{b} | 204 | 139 |
| #6 | - | - | {c}- | - | - | - | - | - | - | - | 280 | 182 | 139 |
| #7 | - | - | - | - | - | - | - | - | - | - | 282 | 173 | 140 |
| #8 | - | - | - | - | - | - | - | - | - | - | - | - | 60 |
| #9 | - | - | - | - | - | - | - | - | - | - | - | - | 135 |
| Average±sn-1(°C) | - | 391 | 201±28 | 187±10 | 418±74 | 871±128 | 761±117 | 227±31 | 207±18 | 271±48 | 290±14 | 194±22 | 137±3 |
| DNB(Departure from nucleate boiling) | - | 154 | 176±2 | 187±10 | 180±7 | 184 | 180±5 | 171±7 | 181±3 | 215±22 | 178±5 | 178±9 | No |
| Coolant temperature; prepulse (°C) | 21 | 16 | 20 | 22 | 18 | 17 | 22 | 21 | 24 | 24 | 22 | 21 | 21 |
| ; peak (°C) | 39 | 42 | 24 | 26 | 47 | 35 | 34 | 43 | 53 | 45 | 58 | 28 | 26 |
| Heat up rate(ms) to Tmax | - | 6.1 | 2.19±0.50 | 4.69±0.82 | 7.44±0.70 | 19.5±4.1 | 38.5±43 | 3.68±0.54 | 4.21±1.15 | 4.41±1.18 | 5.34±1.04 | 2.95±0.39 | 1.20±0.09 |
| Time to quench; tq (s) | - | 0.079 | 0.080±0.01 | 0.062±0.01 | 0.129±0.05 | {i} | {i} | 0.068±0.01 | 0.068±0.04 | 0.056±0.020 | 0.083±0.02 | 0.060±0.02 | 0.11±0.01 |
| Temp.drop ΔT(Tmax-Tp);(°C) | - | 269 | 96±28{d} | 85±11 | 301±80 | 766±33 | 661±165 | 110±37 | 94±17 | 158±45 | 174±16 | 94±22 | 28±2 |
| Cladding wall; min (mm) | 0.355 | 0.347 | 0.320 | 0.261 | 0.154 | 0.000{e} | 0.010 | 0.347 | 0.340 | 0.330 | No PIE | 0.355 | 0.256 |
| Cladding wall; max (mm) | 0.427 | 0.394 | 0.419 | 0.388 | 0.540 | 0.671 | 0.652 | 0.416 | 0.408 | 0.412 | | 0.413 | 0.412 |
| Fuel meat thickness; min (mm) | 0.427 | 0.491 | 0.426 | 0.427 | 0.447 | 0.565 | 0.578 | 0.423 | 0.450 | 0.442 | | 0.462 | 0.433 |
| Fuel meat thickness; max (mm) | 0.549 | 0.554 | 0.610 | 0.587 | 0.620 | 1.078 | 1.125 | 0.558 | 0.554 | 0.560 | | 0.543 | 0.556 |
| Fuel plate thickness; min (mm) | 1.247 | 1.261 | 1.270 | 1.148 | 1.058 | 0.560 | 0.795 | 1.233{f} | 1.206 | 1.224{f} | | 1.240 | 1.235 |
| Fuel plate thickness; max (mm) | 1.267 | 1.289 | 1.330 | 1.21 | 1.440 | 1.515 | 1.549 | 1.258 | 1.274 | 1.261 | | 1.260 | 1.253 |
| Maximum bowing (mm) | 0.11±0.03 | 0.43±0.38 | None | None | 1.2±0.85 | 6.4±0.18 | 2.7±1.2 | 0.53±0.16 | 0.12±0.11 | 0.14±0.07 | | 0.11±0.07 | 0.22±0.14 |
| Failure (F) / No Failure (NF) | NF | F | NF | NF | F | F | F | F | F | F | F | NF | NF |
| Failure mode | | Crack | | | Crack | Cladding melt | Cladding melt | Crack | | | | | |
| Findings in PIE{g} | | IC(1),PT(1) | | | IC(3) | PT(2) CS, CM | IC(1), PT(1) CS, CM | IC(1)PT(1) HS(1) | IC(2),PT(2) | IC(1),PT(1) HS(1) | PT(3) | | |

{a} Thermocouple (T/C) malfunctioned
{b} Two temperature peaks
{c} No thermocouples(T/C's) welded
{d} Temperature drop of 72°Coccurred due to quench at thermocouple location #5

{e} No cladding wall due to significant aluminum agglomeration and denudation
{f} Thickness reduction due to hot spot was not taken into consideration
{g} IC:Incipient crack(number of observations), PT: Through-plate crack, HS: Hot spot, CS: Fuel core separation, CM: Aluminum cladding melt
{i} Time to quench is hard to define because of cladding melt.

3.3 In-core behavior

The in-core behavior of the B&W fuel (one T/C) was the main subject of the discussion.

(1) The onset of the DNB versus the deposited energy

The onset of the DNB, namely the initiation of the film boiling should be important parameter affecting the occurrence of the quench failure. After the DNB, the fuel plate was rapidly heated due to a poor heat conductance from the Al-cladding surface to the coolant. At a local point, the Al-cladding was covered with a vapor due to the high temperature and the vaporized hydrogen could start to interact with the components (Al, Mg) of the Al-cladding. If the hydrogen precipitated into the Al- cladding matrix, the hardening of the cladding would occur. In **Fig. 5**, the onset of the DNB in the B&W fuel is shown as a function of deposited energy. The references are also included. It is interested in mentioning that the DNB did not occur below the energy deposition around 50 cal/g・fuel plate. Above the level but not specified, the DNB should occur irrespective to the fuel failure. The DNB temperature from the references was about $182\pm15$ deg. C. At the energy deposition of 115 cal/g・fuel, the B&W fuel had the DNB at 154 deg. C, the lowest value among the references. This difference however might be not significant. In the figure, two data points having no DNB are shown. First was the reference used in Ex. 508-12 (32cal/g・fuel plate), where the test specimen had the PCST of $137\pm3$deg. C. The second was the reference used in Ex. 508-14(191 cal/g・fuel plate), where the test specimen had PCST of $90\pm9$ deg. C. As to the case, the specimen could not have the DNB because of the heat up rate having the magnitude of 0.0141 deg. C/ms, 1/500 times slower than others (7 deg. C/ms). It is worth to mentioning that all fuels having DNB failed above the 94 cal/g・fuel plate.

(2) The onset of the DNB versus the PCST

As shown in **Fig.6**, the onset of the DNB is plotted to the PCST. After DNB, the DNB temperature of each specimen was almost the constant. The B&W fuel had the lowest level among the fuels having DNB.
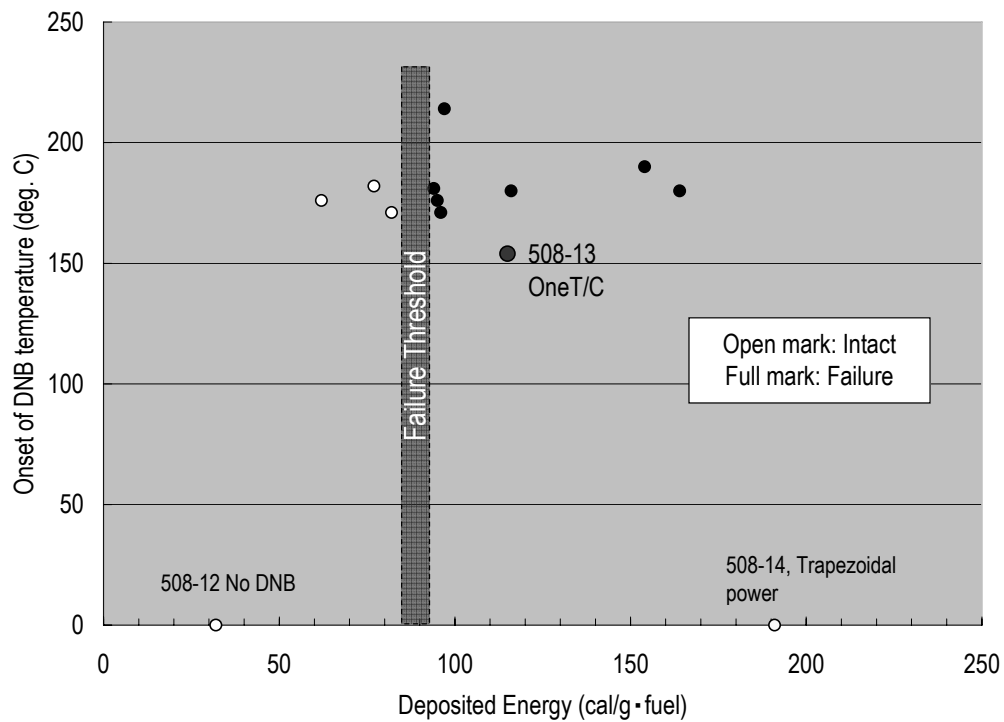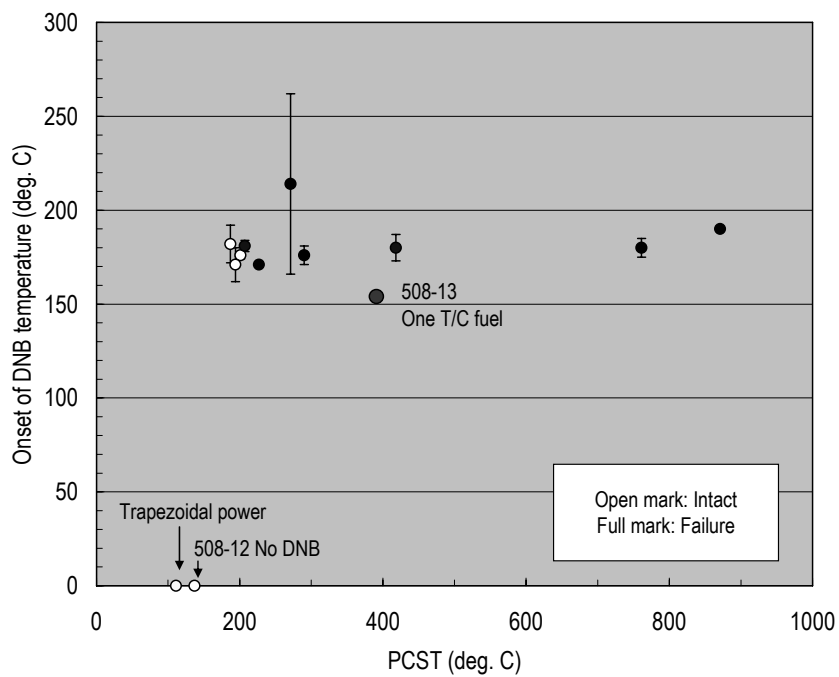
Fig. 5 The onset of the DNB temperature as a function of deposited energy



Fig. 6 The onset of the DNB temperatures as a function of the PCST

(3) The PSCT versus the energy deposition

In **Fig.7**, the B&W fuel and the CERCA (no T/C) fuel are plotted together with the references. The deposited energy for the B&W fuel was 115 cal/g・fuel plate and that for the CERCA fuel was 98 cal/g・fuel plate. The data point of the CERCA was put on the horizontal line due to no T/C. In order to understand the mechanism of the quench failure, the energy deposition should not take an important role because the quench failure was strongly attributed to the time to quench tq and the temperature difference ΔT. This kind of the plotting is very convenient to prepare a tentative failure map but not practical for considering the mechanism of the failure.
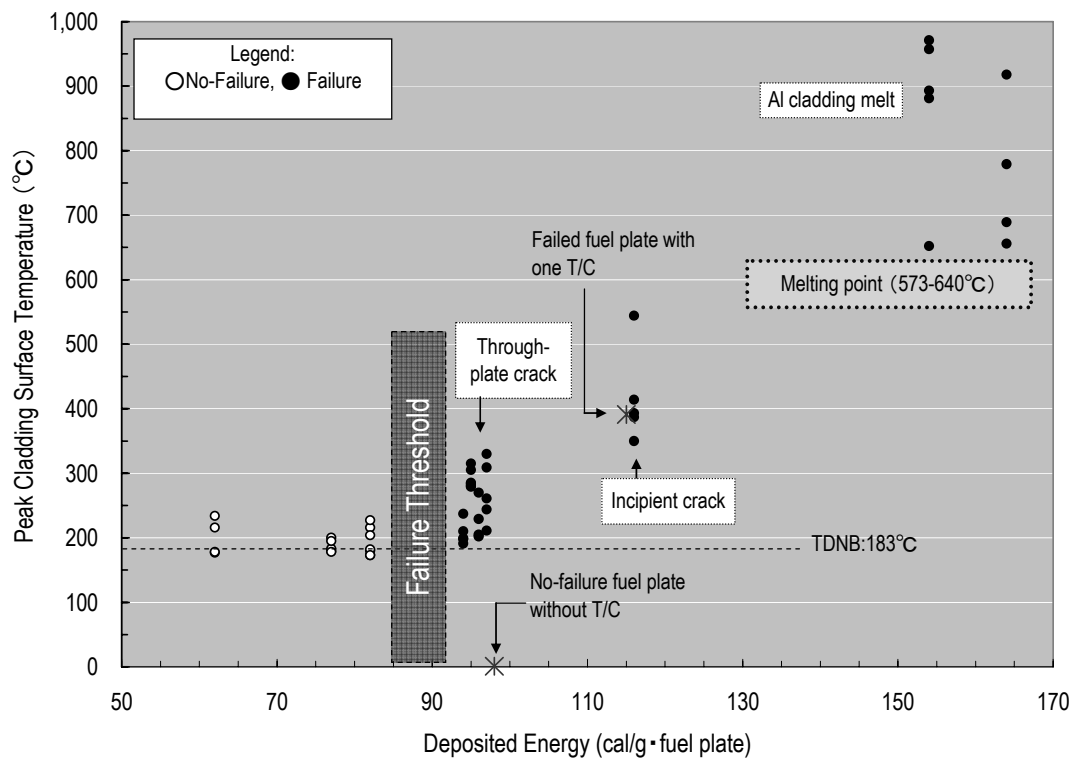
Fig.7 The PCST as a function of the deposited energy. The test specimen with one T/C and that with no T/C are shown by the symbol (*). The latter case showed only the energy deposition due to no T/C.

(4) The temperature drop versus the PCST

The temperature drop ΔT or simply ΔT is one of the important parameters related to the quench failure mechanism, because the thermal stress is given by $\alpha \times E \times \Delta T$, where α is the thermal expansion coefficient , E the Young's modulus and ΔT the temperature drop. As shown in **Fig. 8**, ΔT is revealed to have a linear relationship to

the PCST except for the Ex.508-14, trapezoidal pulse[1]. The reason for the linearity is that ΔT is given by PCST-Tp (quench temperature) and Tp is, as shown in **Fig.9** almost the constant (109±10deg. C from the average of 52 data points), therefore the ΔT has a linear relationship to the PCST. This fact implies us that when the PCST distributes with the uneven temperature profiles, the ΔT (that is, the thermal tensile stress) will be straightforwardly projected the profiles.
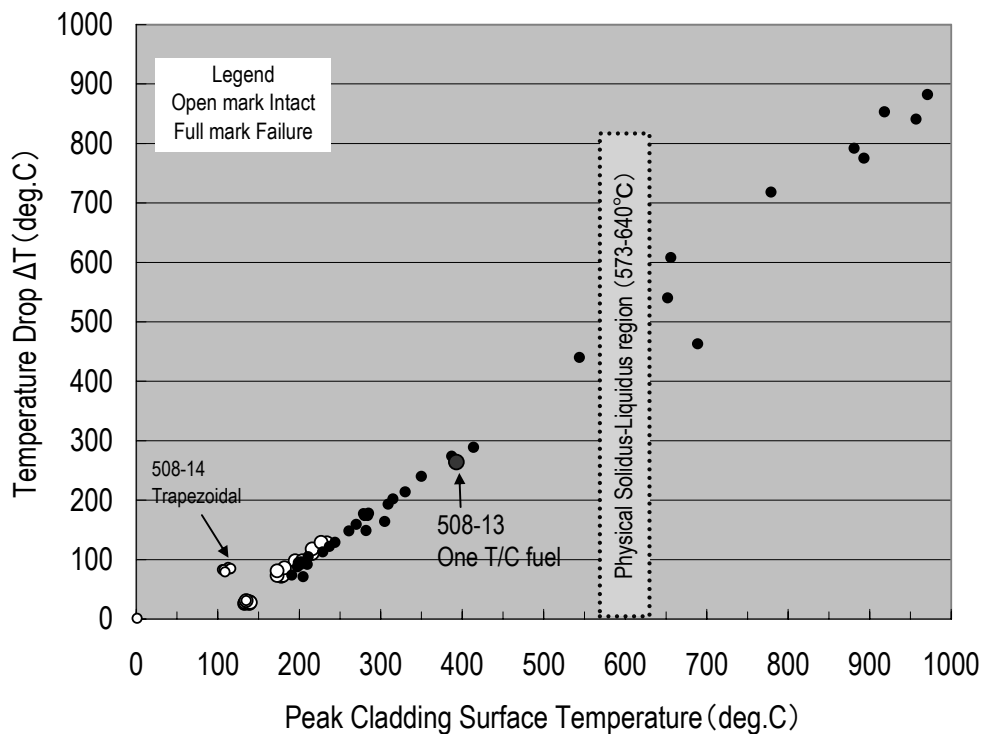


Fig.8 The temperature drop ΔT as a function of the PCST

---

[1]  During the trapezoidal pulse in Ex.508-14, the 4.8g/cc test specimen had the PCST of 111±4 deg. C (no DNB) and quenched to Tp of 27±3deg.C. The small magnitude of the Tp was due to very slow quench by 15±1s. Usually the time to quench was <1s.
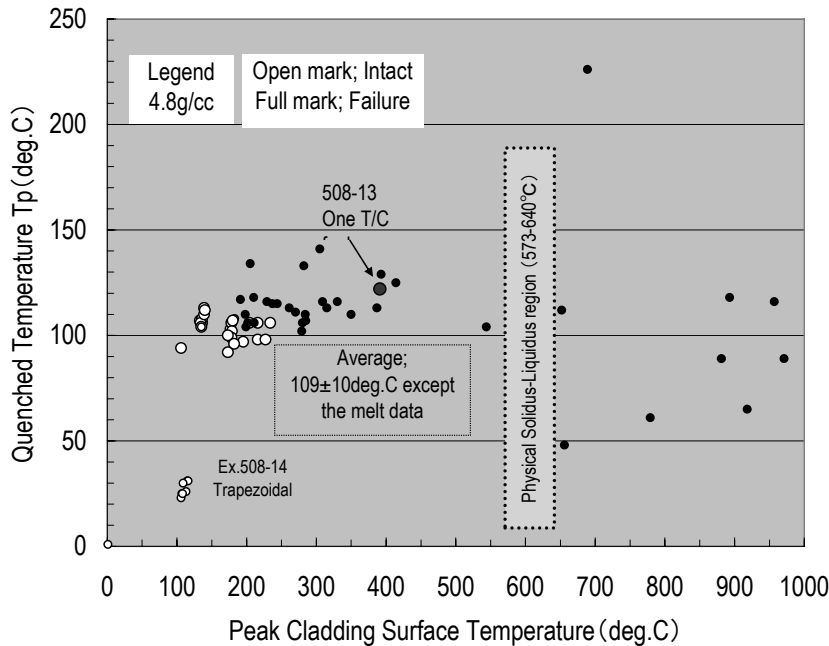
Fig.9 Quench temperature Tp as a function of the PCST. Almost the data, except for the trapezoidal and melt data points, were quenched from the PCST to around the saturation temperature (Tsat, 100deg.C). Experimentally Tp was 109±10deg. C, estimated from the average of 52 data points.

## 3.4 Failure threshold

In the previous section, the author stressed the point that the linearity existed between the ΔT and the PCST. This fact is not new because the author reported this phenomenon in the previous report [4]. In that case, the existence of the uneven temperature profiles was estimated well by the readings from the individual T/C's. However, it was hard to do so by the present B&W fuel because of one T/C. For the reader's more understanding, the author will show the transient temperature in the B&W fuel in **Fig. 10.** In Ex.508-13, the test specimen at the T/C#1 was locally heated from 16deg. C to DNB (154deg. C), and the specimen was continuously heated to the PCST by 391 deg. C. Then, it received the quenching to 122deg. C. Observed ΔT was 269deg. C and tq was 0.079s.
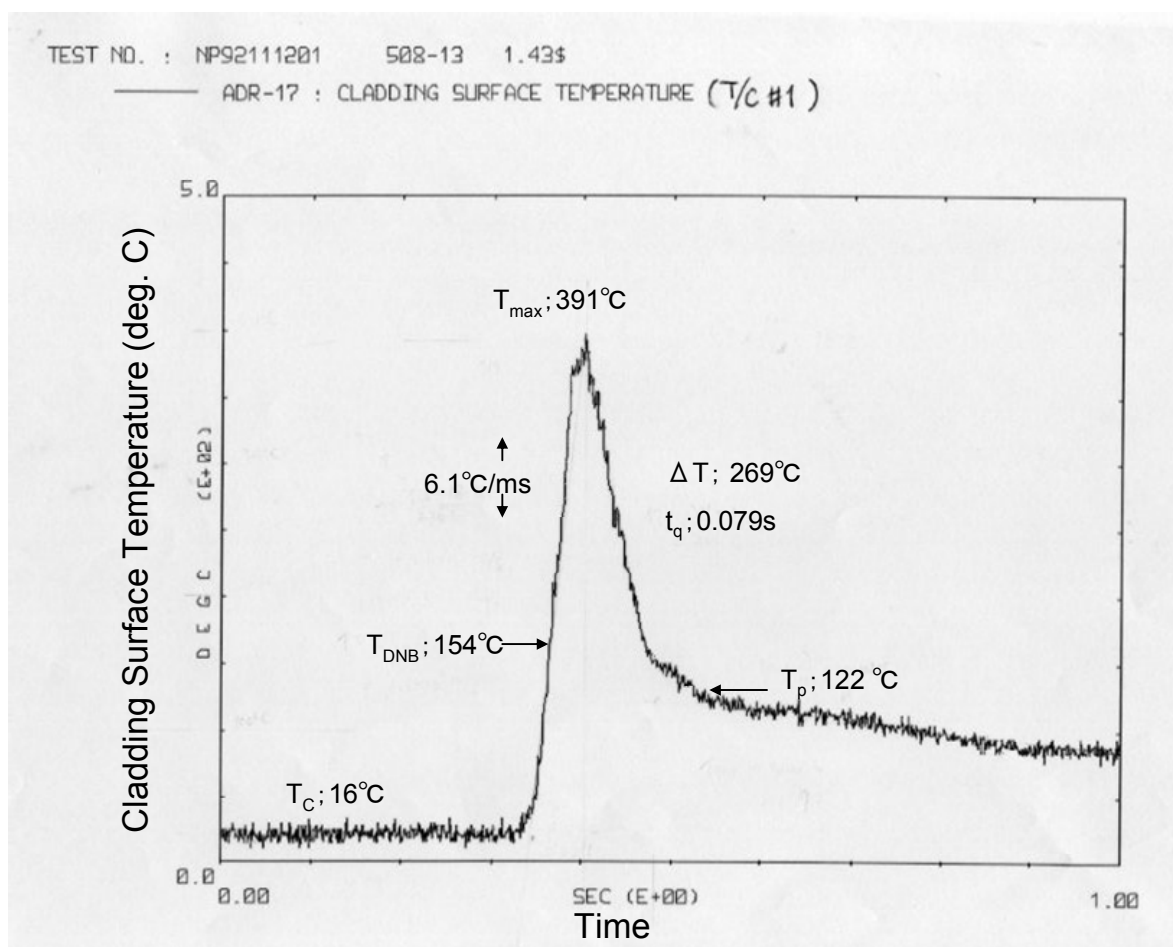
Fig.10 The cladding surface temperature obtained from the T/C#1(solid line) as a function of time; The temperature of the test specimen studied in experiment 508-13(115 cal/g・fuel plate). The test specimen failed.

The two parameters should not be separated because the thermal tensile stress was changed depending on the time-dependent physical factors such as the stress relaxation and the stress recovery. The temperature drop $\Delta T$ and tq are therefore simultaneously plotted in **Fig.11**. Here, the author added the data from the low density fuels (<4.8g/cc) [4]. It is clear that the quench failure can occur under the high temperature drop ($\Delta T$ >94deg. C) , combined to the low time to quench (tq<0.13s). The fuel failure occurred in the B&W test specimen would follow the mechanism well.
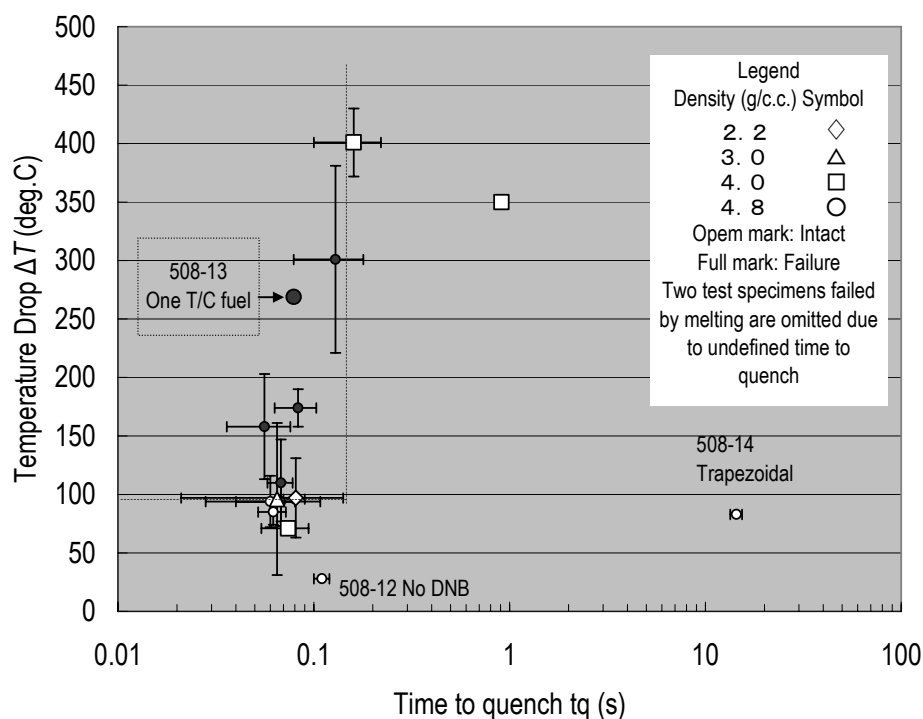
Fig.11 The temperature drop ΔT as a function of the time to quench. Two data failed
by the cladding melt are omitted due to the difficulty to find the tq. Test specimen
having the high temperature drop (ΔT>94deg. C) and that having the low time to
quench (tq<0.13s), failed by the through-plate or the incipient cracking. The B&W fuel
(Ex.508-13) also included the failure region.

3.5 Dimensional stability

During the course of the PIE, the plate bow was determined by the thickness gauge,
inserted into the gap between the test specimen and the molding board. The plate
thickness and the thickness of Al-3wt%Mg cladding were determined by the enlarged
microphotographs cut from the test specimens.

(1) Fuel bow

The magnitude of the plate bow, namely the closure rate of the coolant gap is shown in
**Fig. 12**. The maximum (or the worst) and minimum bows per fuel plate are plotted as a
function of the PCST, because the bow was usually attributed to the uneven
temperature profiles that occurred across the fuel plate. The bow during fabrication
was negligible, that is, almost zero. All data points are increased linearly with an
increase in the PCST.

From the licensing point of view, the channel gap of the JRR-3 was designed to be 2.38mm (A in the figure) and was recommended to operate with a coolant temperature below 228 deg. C (B). Within the experimental scope, the worst bow below 228 deg. C was 15% (0.4mm); however, almost all the data was within 4% (0.1mm). For the B&W fuel, the worst bow was 34% at the elevated temperature of 391 deg. C (>228 deg. C). Not shown in the figure, the worst bow of the CERCA fuel was 6%.

The bow at the elevated temperature was of course significant. As important criteria for the safety licensing was the blistering temperature, that is, 400 deg. C for engineering blistering and 520 deg. C for physical blistering. The experimental showed that the bow was 86% (2.1mm at 492 deg. C) for the former and 110% (2.6mm at 553 deg. C) for the latter. Namely, the coolant channel was closed completely at the temperature level of the latter. This is the main reason why JRR-3 or JMTR core must be operated under the coolant temperature below 228 deg. C. Hypothetically when the cladding was melt, the value was worst at the magnitude of 200% (6.58mm at 999 deg. C). The numeral is not the realistic case.
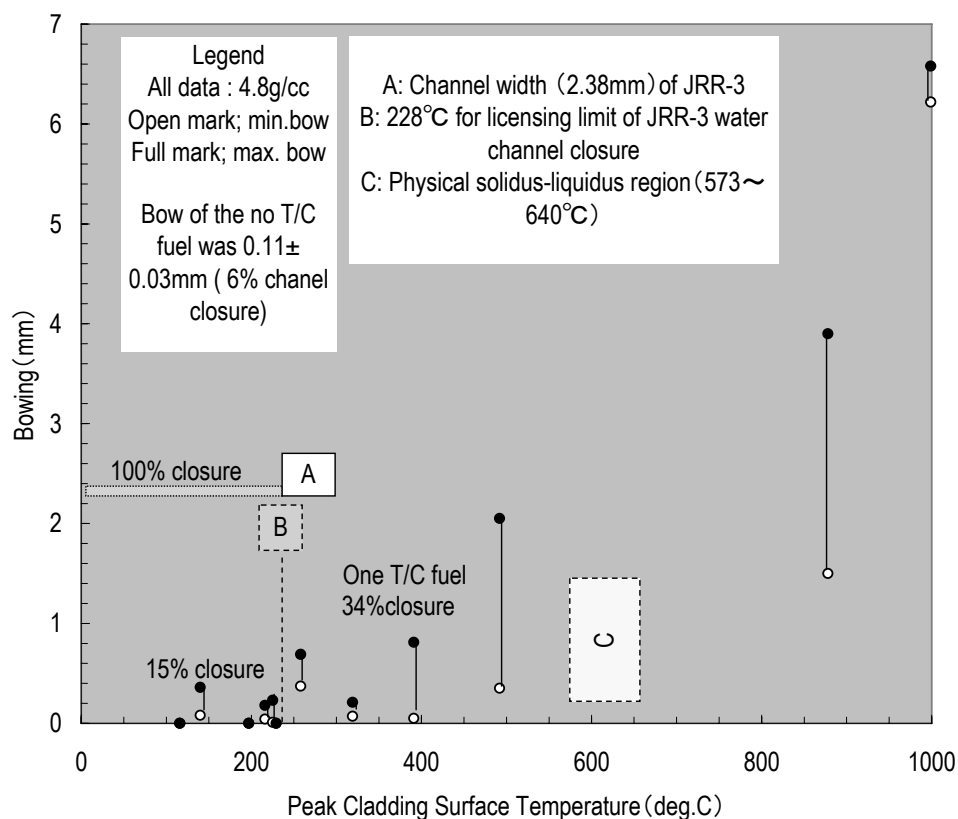
Fig.12 The bow for the test specimens and 4.8g/cc references. The maximum bow in the fuel plate is shown by the solid (full) symbol and the minimum bow is shown by the open symbol. As important indices, the channel width of JRR-3 fuel (2.38mm, A), the licensing limit temperature (228 deg. C, B), and the melting regions (573～640 deg. C, C) are shown. All test specimens, if they exceeded about 182±15deg. C, had a DNB.

(2) Residual strain

The residual strain was obtained from the metallographic pictures cut from the test specimen. Looking over the picture, the maximum and the minimum thickness part was chosen. The data was repeatedly sampled from the different T/C locations. When the measured value was larger or smaller than that of the original, the author denoted it as the swelling or the shrinkage. The value tended to have a significant error band when the place had a large bow. **Fig.13** shows the residual strain for the plate thickness. It is important to say that almost all the data prior to the blistering temperature was shrunk having the error band within ±5%. At the elevated temperature (>400 deg. C),

the CS514819 specimen (Ex. 508-3, failure) had the high value of about 30%. The residual strain for the B&W fuel was 1.5% for the maximum and -1.7% for the minimum. It was the small in the magnitude but swelled partly and shrunk partly. The residual strain for CERCA fuel was -0.2% for the maximum and -1.8% for the minimum. It was also the small in the magnitude but shrunk by the action of the thermal tensile stress. To make the data plotting possible, the author assumed the PCST of CERCA fuel as 350 deg. C. There is no realistic reason to that assumption.
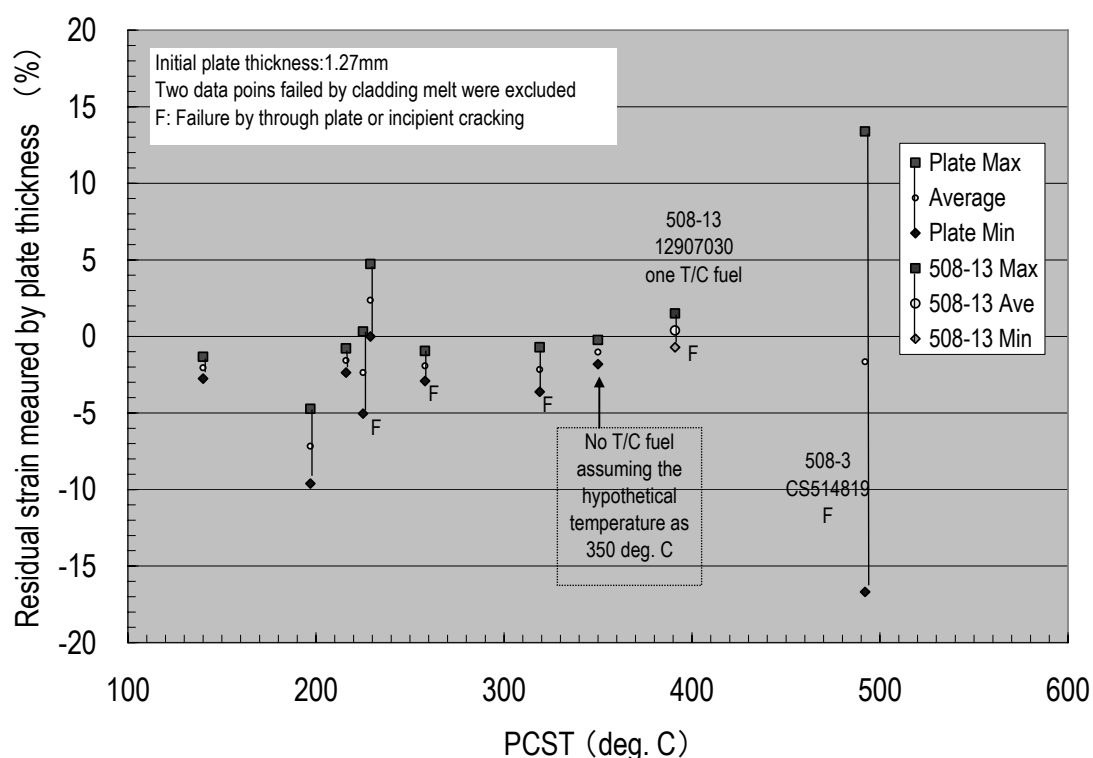


Fig. 13 The residual strain determined by the plate thickness. The nominal initial thickness of the fuel plate was 1.27mm. All data consisted of 4.8g/cc silicide fuel. The fuels failed by the quench are denoted by the symbol F. Tentatively, the residual strain of the CERCA fuel was plotted at the PCST of 350 deg. C.

3.6 The microstructure of the B&W fuel

The B&W fuel was cut in longitudinal direction or in cross sectional one along the T/C. This cutting was aimed at associating the fuel microstructure with the local temperature. After the cutting, the epoxy resin was mounted to the cut specimen for the polishing. The sound papers up to #1000 were continuously used at time interval from 20 to 30 min. each. In the last stage a buff polishing for 30 minutes was added. The fuel microstructure was examined first under as-polished condition. Subsequently the

cut specimen was immersed into the chemical solution made of 1 volumetric percent (*vol*. %) of HF, 9 *vol*. % of $HNO_3$ and pure water for time about 5-10s.This preparation was for examining the grain structure, and so on.

Two typical fuel microstructures were prepared from the B&W fuel. First is shown in **Photo.2.** The upper part of the photograph was taken from the T/C#1 (391 deg. C), showing the several through-plates cracking. Despite the high temperature, no interaction occurred between the dispersed $U_3Si_2$ core and the Al-0.3%Fe matrix. Note that the interaction was typical at the elevated temperature after fuel melting [11]. Boundary between the fuel core and the Al-3wt%Mg cladding was smooth. A grain size of the Al-cladding was the same as that of fabrication (15μm). As-fabricated pores did not agglomerate. The lower part of the Photo.2 was taken from the top part of the fuel plate, where the incipient cracking occurred at the no T/C region. Second is shown in **Photo 3.** From the upper part, the occurrence of the hot spot near the T/C#1 is seen. It was usually isolated from the normal quench front and kept the temperature at the local place very hot. The place was markedly annealed and made the cladding very soft. From the bottom part, the significant pitting is seen, which covered the Al-3wt%Mg cladding as well as Al-0.3wt%Fe core matrix to the some extent. The place was around the center part of the fuel plate. It implied that there occurred significant interaction between the Al-cladding and the certain corrosive elements, like hydrogen.
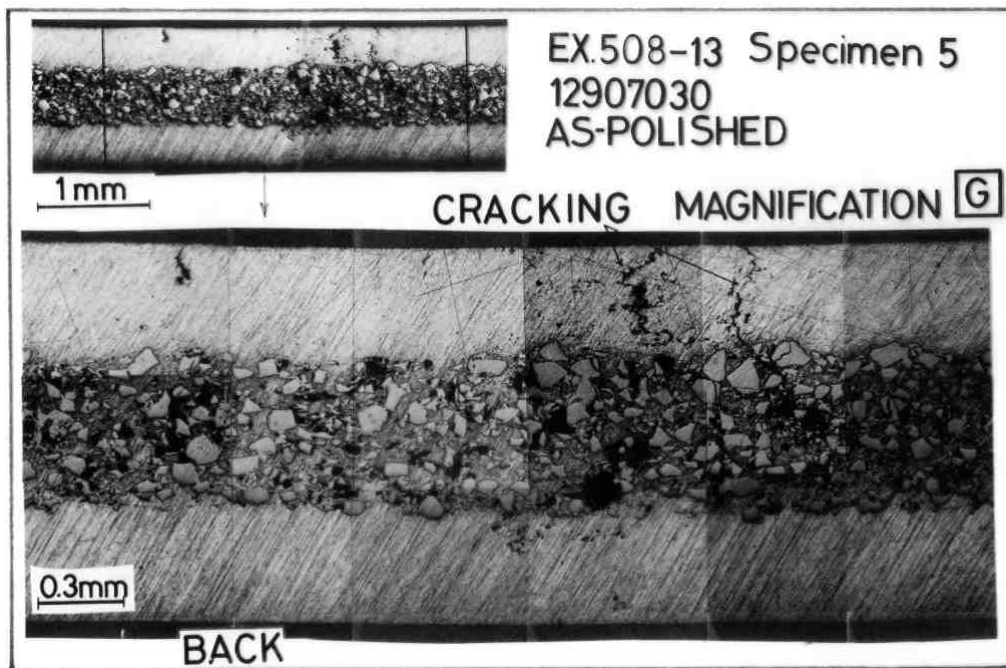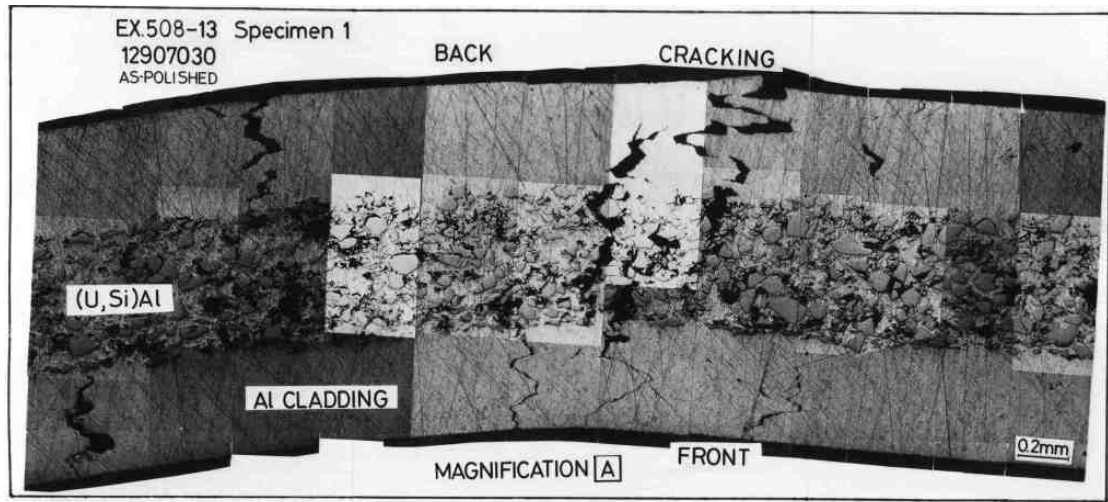
Photo.2 (Top); as-polished microstructure of the B&W fuel (12907030, 4.8g/cc) used in experiment 508-13. The sample was cut from the cross sectional location along the T/C#1 (391 deg. C). Several through-plates cracking are seen at the place, accompanying with a little bow of the plate thickness. (Bottom); as-polished microstructure of the B&W (or one T/C fuel) cut from the fuel top region, where no T/C was spot welded. Several through-plates and incipient cracks were propagated from the Al-cladding outside to the backside.
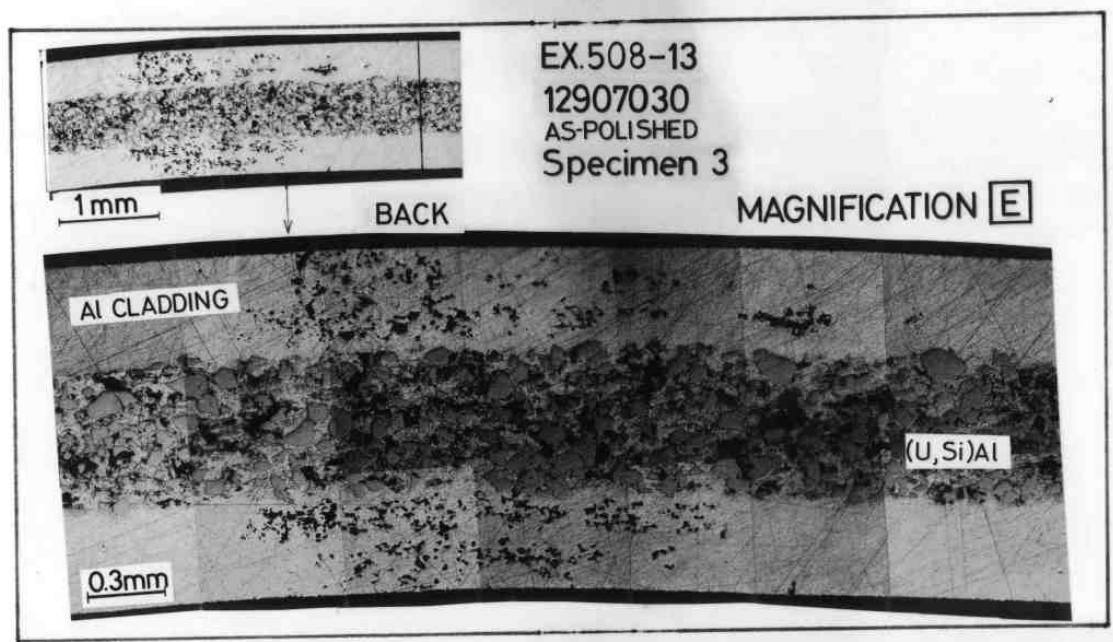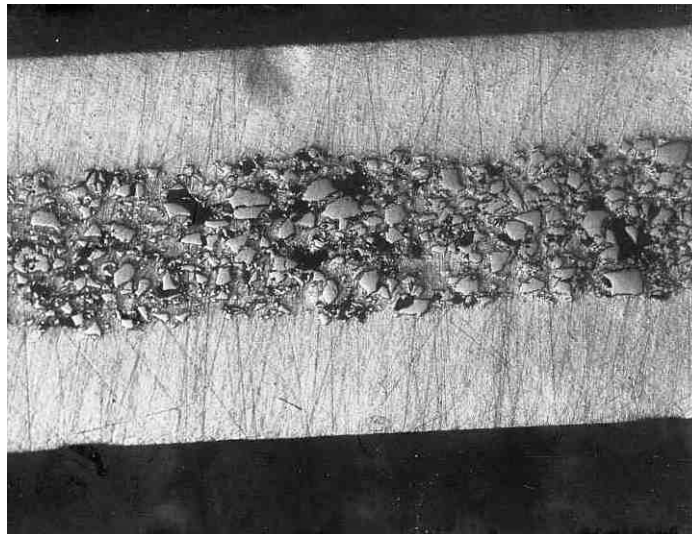
Photo. 3 (Top): the sample was cut from the cross sectional location along the T/C#1 (391 deg. C) of the B&W fuel used in the experiment 508-13. A hot spot indicated by an arrow was observed. (Bottom); many pitting were appeared in the area of the Al-cladding and the Al matrix. The location was the center part of the fuel plate.

**4        Conclusions**

The in-core integrity of the 4.8g/cc silicide fuel fabricated by B&W and that fabricated by CERCA was studied. The inserted reactivity to both fuels was the same as 1.43 dollar, but the resultant deposited energy was 115 cal/.g・fuel plate for the former and 98 cal/.g・fuel plate for the latter. Concluding remarks are as follows.

(1) The onset of the DNB for the B&W fuel was 154 deg. C, which was slightly lower than that of the references (182±18deg. C), but the difference was not significant. The transient temperature observed in the B&W fuel was the similar to that of the references having DNB.

(2) According to the references, the 4.8g/cc silicide fuel caused the quench failure under the high temperature drop ($\Delta$T>94 deg. C), and the low time to quench (tq<0.13s). The B&W fuel had 269 deg. C for $\Delta$T and 0.079s for tq, and failed by the through-plate cracking. On the other hand, CERCA fuel did not fail, masking the details due to no in-core instrument.

(3) The magnitude of the bow for the B&W fuel was 34%. This value was due to the high PSCT of 391 deg. C. The magnitude of the bow for the CERCA fuel was 6%. Taking into consideration that the magnitude of bow had a linear relationship to PCST, the PCST of the CERCA fuel might be lower than that of the B&W fuel.

(4) The residual strain was determined by the change of plate thickness. For the B&W fuel it was ranged from 1.5% to -1.7%. The fuel plate swelled partly and shrunk partly. For the CERCA fuel it was ranged from -0.2% to -1.8%. The fuel plate was shrunk Almost all the data including the B&W and the CERCA showed that the residual strain was in the range within ±5%.

(5) As the typical damage observed in the B&W fuel was the hot spot near the T/C#1 and a lot of pitting near the center part.

**References**

[1]    K. Yanagisawa, T. Fujishiro, O. Horiki, K. Soyama, H. Ichikawa, T. Kodaira: *Dimensional Stability of Low-Enriched Uranium Silicide Plate-Type Fuel for Research Reactors at Transient Conditions*, J. Nucl. Sci. Technol., **29** [3], p.233 (1992).

[2]    K. Yanagisawa, T. Fujishiro, O. Horiki, K. Soyama, H. Ichikawa, T. Kodaira: *Transient Behavior of Low Enriched Uranium Silicide Plate-Type Fuel for Research Reactors during RIA Conditions*, J. Nucl. Sci. Technol., **30** [8], p.741 (1993).

[3]    K. Yanagisawa, T. Fujishiro : *Transient Behavior of Low Enriched Uranium Silicide Miniplate Fuel Under A Triplet Configuration,* J. Nucl. Sci. Technol., **32** [9], p.889 (1995).

[4]    K. Yanagisawa: *Transient Behaviour of Low Enriched Uranium Silicide Plate-Type Fuel for Research Reactors during Reactivity Initiated Accident.* Int. J. of Nucl. Energy Sci. and Technol., Vol **.4**, No.2, pp.97-110 (2008).

[5]    K. Yanagisawa: *Transient Behaviour of Low Enriched Uranium Silicide Plate-Type Fuel for Research Reactors during Reactivity Initiated Accident,* International Topical Meeting on Safety of Nuclear Installations   TOPSAFE 2008, Area 3; Research Reactors A3-035, Palace Hotel, Dubrovnik, Croatia (2008).

[6]    K. Yanagisawa: *Transient Behaviour of Low Enriched Uranium Silicide Plate-Type Fuel for Research Reactors during Reactivity Initiated Accident,* International Symposium on the Peaceful Application of Nuclear Technology in GCC Countries, November 3-5 2008, Jeddah, Saudi Arabia (2008).

[7]    K. Yanagisawa: *Study on Silicide Fuel Behavior during RIA*. International Congress on Advances in Nuclear Power Plants (ICAPP2009), held on May 10-14, at the Keio Plaza Hotel, Shinjuku, Tokyo, Japan. Paper 9040 (2009).

[8]    K. Yanagisawa: *Study on Silicide Fuel Behavior during Power Transient,* TOPFUEL2009, Session 5.02 In-pile Behavior –I, Paper No. 2034, pp.1226-1235, held on 6-10 September, Place de la Porte Maillot, Paris, France (2009).

[9]    K. Yanagisawa: *Study on In-pile Performance of Silicide Fuel under Power Transient,* 31st International Meeting on RERTR (Reduced Enrichment for Research and Test Reactors) ,1-5 November, Kempinski Hotel Beijing Lufthansa Center, Beijing, China (2009)

[10] K. Yanagisawa, K. Soyama, H. Ichikawa, T. Nemoto, O. Hoshino, H. Uno, M. Umeda, T. Suzuki, H. Kanazawa, Y. Kimura, and H. Mimura: *Technical Report; Technical Development on the Silicide Plate-type Fuel Experiment at Nuclear Safety Research Reactor*, JAERI-M 91-114(1991) <In Japanese>.

[11] K. Yanagisawa: *Interaction of Molten Aluminum Cladding with $U_3Si_2$ Particles under Transient Conditions,* JAERI-M 93-129 (1993).

# 国際単位系（SI）

## 表1．SI基本単位

| 基本量 | SI基本単位 名称 | 記号 |
|---|---|---|
| 長　　さ | メートル | m |
| 質　　量 | キログラム | kg |
| 時　　間 | 秒 | s |
| 電　　流 | アンペア | A |
| 熱力学温度 | ケルビン | K |
| 物　質　量 | モル | mol |
| 光　　度 | カンデラ | cd |

## 表2．基本単位を用いて表されるSI組立単位の例

| 組立量 | SI基本単位 名称 | 記号 |
|---|---|---|
| 面　　　　　積 | 平方メートル | m² |
| 体　　　　　積 | 立法メートル | m³ |
| 速　さ，速　度 | メートル毎秒 | m/s |
| 加　　速　　度 | メートル毎秒毎秒 | m/s² |
| 波　　　　　数 | 毎メートル | m⁻¹ |
| 密度，質量密度 | キログラム毎立方メートル | kg/m³ |
| 面　積　密　度 | キログラム毎平方メートル | kg/m² |
| 比　　体　　積 | 立方メートル毎キログラム | m³/kg |
| 電　流　密　度 | アンペア毎平方メートル | A/m² |
| 磁界の強さ | アンペア毎メートル | A/m |
| 量濃度 (a)，濃度 | モル毎立方メートル | mol/m³ |
| 質　量　濃　度 | キログラム毎立法メートル | kg/m³ |
| 輝　　　　　度 | カンデラ毎平方メートル | cd/m² |
| 屈　折　率 (b) | （数字の）1 | 1 |
| 比　透　磁　率 (b) | （数字の）1 | 1 |

(a) 量濃度（amount concentration）は臨床化学の分野では物質濃度（substance concentration）ともよばれる。
(b) これらは無次元量あるいは次元1をもつ量であるが、そのことを表す単位記号である数字の1は通常は表記しない。

## 表3．固有の名称と記号で表されるSI組立単位

| 組立量 | SI組立単位 名称 | 記号 | 他のSI単位による表し方 | SI基本単位による表し方 |
|---|---|---|---|---|
| 平　面　角 | ラジアン (b) | rad | 1 (b) | m/m |
| 立　体　角 | ステラジアン (b) | sr (c) | 1 (b) | m²/m² |
| 周　波　数 | ヘルツ (d) | Hz | | s⁻¹ |
| 力 | ニュートン | N | | m kg s⁻² |
| 圧　力，応　力 | パスカル | Pa | N/m² | m⁻¹ kg s⁻² |
| エネルギー，仕事，熱量 | ジュール | J | N m | m² kg s⁻² |
| 仕事率，工率，放射束 | ワット | W | J/s | m² kg s⁻³ |
| 電荷，電気量 | クーロン | C | | s A |
| 電位差（電圧），起電力 | ボルト | V | W/A | m² kg s⁻³ A⁻¹ |
| 静　電　容　量 | ファラド | F | C/V | m⁻² kg⁻¹ s⁴ A² |
| 電　気　抵　抗 | オーム | Ω | V/A | m² kg s⁻³ A⁻² |
| コンダクタンス | ジーメンス | S | A/V | m⁻² kg⁻¹ s³ A² |
| 磁　　　　　束 | ウェーバ | Wb | Vs | m² kg s⁻² A⁻¹ |
| 磁　束　密　度 | テスラ | T | Wb/m² | kg s⁻² A⁻¹ |
| インダクタンス | ヘンリー | H | Wb/A | m² kg s⁻² A⁻² |
| セルシウス温度 | セルシウス度 (e) | ℃ | | K |
| 光　　　　　束 | ルーメン | lm | cd sr (c) | cd |
| 照　　　　　度 | ルクス | lx | lm/m² | m⁻² cd |
| 放射性核種の放射能 (f) | ベクレル (d) | Bq | | s⁻¹ |
| 吸収線量, 比エネルギー分与, カーマ | グレイ | Gy | J/kg | m² s⁻² |
| 線量当量, 周辺線量当量, 方向性線量当量, 個人線量当量 | シーベルト (g) | Sv | J/kg | m² s⁻² |
| 酸　素　活　性 | カタール | kat | | s⁻¹ mol |

(a) SI接頭語は固有の名称と記号を持つ組立単位と組み合わせても使用できる。しかし接頭語を付けた単位はもはやコヒーレントではない。
(b) ラジアンとステラジアンは数字の1に対する単位の特別な名称で、量についての情報をつたえるために使われる。実際には、使用する時には記号rad及びsrが用いられるが、習慣として組立単位としての記号である数字の1は明示されない。
(c) 測光学ではステラジアンという名称と記号srを単位の表し方の中で、そのまま維持している。
(d) ヘルツは周期現象についてのみ、ベクレルは放射性核種の統計的過程についてのみ使用される。
(e) セルシウス度はケルビンの特別な名称で、セルシウス温度を表すために使用される。セルシウス度とケルビンの単位の大きさは同一である。したがって、温度差や温度間隔を表す数値はどちらで表しても同じである。
(f) 放射性核種の放射能（activity referred to a radionuclide）は、しばしば誤った用語で"radioactivity"と記される。
(g) 単位シーベルト（PV,2002,70,205）についてはCIPM勧告2（CI-2002）を参照。

## 表4．単位の中に固有の名称と記号を含むSI組立単位の例

| 組立量 | SI組立単位 名称 | 記号 | SI基本単位による表し方 |
|---|---|---|---|
| 粘　　　　　　　度 | パスカル秒 | Pa s | m⁻¹ kg s⁻¹ |
| 力のモーメント | ニュートンメートル | N m | m² kg s⁻² |
| 表　面　張　力 | ニュートン毎メートル | N/m | kg s⁻² |
| 角　　速　　度 | ラジアン毎秒 | rad/s | m m⁻¹ s⁻¹=s⁻¹ |
| 角　加　速　度 | ラジアン毎秒毎秒 | rad/s² | m m⁻¹ s⁻²=s⁻² |
| 熱流密度, 放射照度 | ワット毎平方メートル | W/m² | kg s⁻³ |
| 熱容量, エントロピー | ジュール毎ケルビン | J/K | m² kg s⁻² K⁻¹ |
| 比熱容量, 比エントロピー | ジュール毎キログラム毎ケルビン | J/(kg K) | m² s⁻² K⁻¹ |
| 比エネルギー | ジュール毎キログラム | J/kg | m² s⁻² |
| 熱　伝　導　率 | ワット毎メートル毎ケルビン | W/(m K) | m kg s⁻³ K⁻¹ |
| 体積エネルギー | ジュール毎立方メートル | J/m³ | m⁻¹ kg s⁻² |
| 電　界　の　強　さ | ボルト毎メートル | V/m | m kg s⁻³ A⁻¹ |
| 電　荷　密　度 | クーロン毎立方メートル | C/m³ | m⁻³ sA |
| 表　面　電　荷 | クーロン毎平方メートル | C/m² | m⁻² sA |
| 電束密度, 電気変位 | クーロン毎平方メートル | C/m² | m⁻² sA |
| 誘　　電　　率 | ファラド毎メートル | F/m | m⁻³ kg⁻¹ s⁴ A² |
| 透　　磁　　率 | ヘンリー毎メートル | H/m | m kg s⁻² A⁻² |
| モルエネルギー | ジュール毎モル | J/mol | m² kg s⁻² mol⁻¹ |
| モルエントロピー, モル熱容量 | ジュール毎モル毎ケルビン | J/(mol K) | m² kg s⁻² K⁻¹ mol⁻¹ |
| 照射線量（X線及びγ線） | クーロン毎キログラム | C/kg | kg⁻¹ sA |
| 吸　収　線　量　率 | グレイ毎秒 | Gy/s | m² s⁻³ |
| 放　射　強　度 | ワット毎ステラジアン | W/sr | m⁴ m⁻² kg s⁻³=m² kg s⁻³ |
| 放　射　輝　度 | ワット毎平方メートル毎ステラジアン | W/(m² sr) | m² m⁻² kg s⁻³=kg s⁻³ |
| 酵　素　活　性　濃　度 | カタール毎立方メートル | kat/m³ | m⁻³ s⁻¹ mol |

## 表5．SI接頭語

| 乗数 | 接頭語 | 記号 | 乗数 | 接頭語 | 記号 |
|---|---|---|---|---|---|
| 10²⁴ | ヨ　タ | Y | 10⁻¹ | デ　シ | d |
| 10²¹ | ゼ　タ | Z | 10⁻² | センチ | c |
| 10¹⁸ | エクサ | E | 10⁻³ | ミ　リ | m |
| 10¹⁵ | ペ　タ | P | 10⁻⁶ | マイクロ | μ |
| 10¹² | テ　ラ | T | 10⁻⁹ | ナ　ノ | n |
| 10⁹ | ギ　ガ | G | 10⁻¹² | ピ　コ | p |
| 10⁶ | メ　ガ | M | 10⁻¹⁵ | フェムト | f |
| 10³ | キ　ロ | k | 10⁻¹⁸ | ア　ト | a |
| 10² | ヘクト | h | 10⁻²¹ | ゼプト | z |
| 10¹ | デ　カ | da | 10⁻²⁴ | ヨクト | y |

## 表6．SIに属さないが、SIと併用される単位

| 名称 | 記号 | SI単位による値 |
|---|---|---|
| 分 | min | 1 min=60s |
| 時 | h | 1h＝60 min=3600 s |
| 日 | d | 1 d=24 h=86 400 s |
| 度 | ° | 1°=(π/180) rad |
| 分 | ’ | 1’=(1/60)°=(π/10800) rad |
| 秒 | ” | 1”=(1/60)’=(π/648000) rad |
| ヘクタール | ha | 1ha=1hm²=10⁴m² |
| リットル | L, l | 1L=11=1dm³=10³cm³=10⁻³m³ |
| トン | t | 1t=10³ kg |

## 表7．SIに属さないが、SIと併用される単位で、SI単位で表される数値が実験的に得られるもの

| 名称 | 記号 | SI単位で表される数値 |
|---|---|---|
| 電子ボルト | eV | 1eV=1.602 176 53(14)×10⁻¹⁹J |
| ダルトン | Da | 1Da=1.660 538 86(28)×10⁻²⁷kg |
| 統一原子質量単位 | u | 1u=1 Da |
| 天文単位 | ua | 1ua=1.495 978 706 91(6)×10¹¹m |

## 表8．SIに属さないが、SIと併用されるその他の単位

| 名称 | 記号 | SI単位で表される数値 |
|---|---|---|
| バール | bar | 1 bar=0.1MPa=100kPa=10⁵Pa |
| 水銀柱ミリメートル | mmHg | 1mmHg=133.322Pa |
| オングストローム | Å | 1 Å=0.1nm=100pm=10⁻¹⁰m |
| 海里 | M | 1 M=1852m |
| バーン | b | 1 b=100fm²=(10⁻¹²cm)2=10⁻²⁸m² |
| ノット | kn | 1 kn=(1852/3600)m/s |
| ネーパ | Np | SI単位との数値的な関係は、対数量の定義に依存。 |
| ベル | B | |
| デジベル | dB | |

## 表9．固有の名称をもつCGS組立単位

| 名称 | 記号 | SI単位で表される数値 |
|---|---|---|
| エ　ル　グ | erg | 1 erg=10⁻⁷ J |
| ダ　イ　ン | dyn | 1 dyn=10⁻⁵N |
| ポ　ア　ズ | P | 1 P=1 dyn s cm⁻²=0.1Pa s |
| ストークス | St | 1 St =1cm² s⁻¹=10⁻⁴m² s⁻¹ |
| スチルブ | sb | 1 sb =1cd cm⁻²=10⁴cd m⁻² |
| フォト | ph | 1 ph=1cd sr cm⁻² 10⁴lx |
| ガ　ル | Gal | 1 Gal =1cm s⁻²=10⁻²ms⁻² |
| マクスウェル | Mx | 1 Mx = 1G cm²=10⁻⁸Wb |
| ガ　ウ　ス | G | 1 G =1Mx cm⁻²=10⁻⁴T |
| エルステッド (c) | Oe | 1 Oe ≙ (10³/4π)A m⁻¹ |

(c) 3元系のCGS単位系とSIでは直接比較できないため、等号「 ≙ 」は対応関係を示すものである。

## 表10．SIに属さないその他の単位の例

| 名称 | 記号 | SI単位で表される数値 |
|---|---|---|
| キュリー | Ci | 1 Ci=3.7×10¹⁰Bq |
| レントゲン | R | 1 R = 2.58×10⁻⁴C/kg |
| ラド | rad | 1 rad=1cGy=10⁻²Gy |
| レム | rem | 1 rem=1 cSv=10⁻²Sv |
| ガンマ | γ | 1 γ=1 nT=10-9T |
| フェルミ | | 1フェルミ=1 fm=10-15m |
| メートル系カラット | | 1メートル系カラット = 200 mg = 2×10-4kg |
| トル | Torr | 1 Torr = (101 325/760) Pa |
| 標準大気圧 | atm | 1 atm = 101 325 Pa |
| カロリー | cal | 1cal=4.1858J（「15℃」カロリー）, 4.1868J（「IT」カロリー）4.184J（「熱化学」カロリー） |
| ミクロン | μ | 1 μ=1μm=10⁻⁶m |